

Regular Article

Density of Hydroxyl Radicals Generated in an Aqueous Solution by Irradiating Carbon-Ion Beam

Ken-ichiro Matsumoto,*^a Megumi Ueno,^a Ikuo Nakanishi,^a and Kazunori Anzai^{a,b}^aRadio-Redox-Response Research Team, Advanced Particle Radiation Biology Research Program, Research Center for Charged Particle Therapy, National Institute of Radiological Sciences; 4-9-1 Anagawa, Inage-ku, Chiba 263-8555, Japan; and ^bNihon Pharmaceutical University; Saitama 362-0806, Japan.

Received October 23, 2014; accepted December 26, 2014; advance publication released online January 14, 2015

The density of hydroxyl radicals ($\cdot\text{OH}$) produced in aqueous samples by exposure to X-ray or carbon-ion beams was investigated. The generation of $\cdot\text{OH}$ was detected by the electron paramagnetic resonance (EPR) spin-trapping technique using 5,5-dimethyl-1-pyrroline-*N*-oxide (DMPO) as the spin-trapping agent. When the concentration of DMPO is in excess of the generated $\cdot\text{OH}$, the production of DMPO-OH (spin-trapped $\cdot\text{OH}$) should be saturated. Reaction mixtures containing several concentrations (0.5–1685 mM) of DMPO were then irradiated by a 32 Gy 290 MeV carbon-ion beam (C290-beam) or X-ray. C290-beam irradiation was performed at the Heavy-Ion Medical Accelerator in Chiba (HIMAC, National Institute of Radiological Sciences, Chiba, Japan), applying different linear energy transfers (LET) (20–169 keV/ μm). The amount of DMPO-OH in the irradiated samples was detected by EPR spectroscopy. The generation of DMPO-OH increased with the concentration of initial DMPO, displayed a shoulder around 3.3 mM DMPO, and reached a plateau. This plateau suggests that the generated $\cdot\text{OH}$ were completely trapped. Another linear increase in DMPO-OH measured in solutions with higher DMPO concentrations suggested very dense $\cdot\text{OH}$ generation ($>1.7\text{ M}$). Generation of $\cdot\text{OH}$ is expected to be localized on the track of the radiation beam, because the maximum concentration of measured DMPO-OH was 40 μM . These results suggested that both sparse ($\approx 3.3\text{ mM}$) and dense ($>1.7\text{ M}$) $\cdot\text{OH}$ generation occurred in the irradiated samples. The percentage of dense $\cdot\text{OH}$ generation increased with increasing LET. Different types of dense $\cdot\text{OH}$ generation may be expected for X-ray and C290-beams.

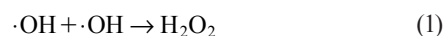
Key words hydroxyl radical; carbon-ion beam; ionizing radiation; EPR spin-trapping; reactive oxygen species; high linear energy transfer

Use of high linear energy transfer (LET) carbon-ion beam cancer therapy is effective against hypoxic tumors; this type of radiation has a lower oxygen effect compared to low LET irradiation, such as X-rays and γ -rays.¹⁾ The Heavy-Ion Medical Accelerator in Chiba (HIMAC, National Institute of Radiological Sciences, Chiba, Japan) has been applied clinically for cancer therapy since 1994 using a 290 MeV/nucleon carbon-ion beam.²⁾ Hypofractionation protocols are being planned for future improvement of carbon-ion beam cancer therapy; such protocols for low-fractionation can decrease anxiety in patients by reducing the repetition of long binding time for positioning. When the fractionation number decreases, the dose per each fraction must be increased to preserve an equivalent effect as conventional protocols. However, generation of higher doses by high LET beams may produce reactive oxygen species (ROS) at non-negligible levels, particularly in normal tissues.

When ionizing radiation, including carbon-ion beams, is delivered to living cells/animals, ROS such as hydroxyl radicals ($\cdot\text{OH}$), superoxide (O_2^-), and hydrogen peroxide (H_2O_2) are produced. Initial generation of $\cdot\text{OH}$ is *via* direct radiolysis of water. Highly reactive $\cdot\text{OH}$ cannot travel long distances, but instead immediately react with other molecules nearby. O_2^- and H_2O_2 are subsequently produced by reaction of these water-derived reactive species with oxygen. Our previous studies^{3,4)} demonstrated evidence supporting the generation of O_2^- and H_2O_2 in aqueous samples by carbon-ion beam irradiation. Because generation of O_2^- and H_2O_2 was associated with

oxygen consumption, the density of such ROS generation depended mainly on the concentration of dissolved oxygen in the irradiated sample. In other words, tissue oxygen concentration may modify the biological results of radiation by ROS generation, a phenomenon known as the “oxygen effect.” However, tissue oxygen concentration, even in normoxic noncancerous tissues ($\text{pO}_2 < 40\text{ mmHg}$)⁵⁾ is much lower compared to the air-equilibrated *in vitro* samples such as what we used in our previous studies.

Assuming that initial generation of $\cdot\text{OH}$ is entirely due to radiolysis of water molecules, the density of generated $\cdot\text{OH}$ in the irradiated sample depends on the density of water molecules and the frequency of ionization on the track of the radiation beam. Generation of $\cdot\text{OH}$ can be assumed to be more frequent than O_2^- and H_2O_2 , and may be localized to the track of the radiation beam. When the distance between two adjacent $\cdot\text{OH}$ becomes sufficiently short, a coupling reaction between the $\cdot\text{OH}$ can generate H_2O_2 without accompanying O_2 consumption (Eq. 1).



A subsequent reaction between $\cdot\text{OH}$ and H_2O_2 can then make O_2^- (Eq. 2).



When the O_2^- and H_2O_2 diffuse away, molecules distant from the site of $\cdot\text{OH}$ generation can then be oxidized by secondary reactions. Therefore, initial generation of $\cdot\text{OH}$ has a signifi-

* To whom correspondence should be addressed. e-mail: matsumok@nirs.go.jp

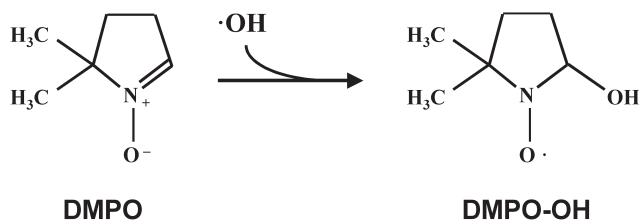


Fig. 1. Detection of $\cdot\text{OH}$ by the EPR Spin-Trapping Technique

DMPO, a spin-trapping agent, behaves as a molecular detector of $\cdot\text{OH}$. DMPO can react with $\cdot\text{OH}$ to produce DMPO-OH, which is the spin-trapped form of $\cdot\text{OH}$. DMPO-OH can be measured by an X-band EPR spectrometer at room temperature.

cant effect in low oxygen and hypoxic environments, particularly in the *in vivo* environment of hypoxic tumors.

In this study, $\cdot\text{OH}$ generated in irradiated samples were detected by the electron paramagnetic resonance (EPR) spin-trapping technique using the spin-trapping agent, 5,5-dimethyl-1-pyrroline-*N*-oxide (DMPO). DMPO reacts with $\cdot\text{OH}$ to produce DMPO-OH (spin trapped $\cdot\text{OH}$), which is a relatively stable nitroxyl radical form (Fig. 1) that can be detected by an EPR spectrometer at room temperature. To detect $\cdot\text{OH}$ efficiently, the concentrations of DMPO, *i.e.*, the molecular detector, must be in excess than that of the $\cdot\text{OH}$ generated in the irradiated sample. Aqueous reaction mixtures containing several concentrations of DMPO were prepared, and the concentration of DMPO-OH was measured after irradiation by an X-ray or carbon-ion beam; the level of $\cdot\text{OH}$ generated in the aqueous reaction mixtures was then determined.

Experimental

Chemicals and Sample Preparation 5,5-Dimethyl-1-pyrroline-*N*-oxide (DMPO) was purchased from LABOTEC Co. (Tokyo, Japan). Other chemicals were of analytical grade. Phosphate buffer (PB, 100 mM, pH 7.0), containing 0.05 mM diethylenetriaminepentaacetic acid (DTPA), was prepared with deionized water (deionized by the Milli-Q system, Merck Millipore, Billerica, MA, U.S.A.). Reaction mixtures containing several concentrations (0.5–1685 mM) of DMPO were prepared.

X-Ray Irradiation For X-ray irradiation, a 150 μL aliquot of the reaction mixture was transferred into a polyethylene microtube, and kept on ice until irradiation. X-ray irradiation was performed using the PANTAK 320S (Shimadzu, Kyoto, Japan) at room temperature. The effective energy of the X-ray was 80 keV under the following conditions: X-ray tube voltage, 200 kV; X-ray tube current, 20 mA; thickness and materials of the pre-filter; 0.5 mm copper and 0.5 mm aluminum. The reaction mixtures were irradiated with 32 Gy at a dose rate of 3.3 Gy/min.

Carbon-Ion Beam Irradiation A 350 μL aliquot of reaction mixture was transferred into a thin, flat, polyethylene bag, and kept on ice until irradiation. The polyethylene bag was attached to a flat acrylic sample holder and irradiated with a 290 MeV/nucleon carbon-ion beam (C290-beam) using the HIMAC at room temperature. A schematic drawing of the experimental setup is shown in Fig. 2. Irradiation experiments at several LET conditions (20, 40, 60, 80, and 169 keV/ μm) were performed. The calculated LET at the surface of the sample was based on the thickness of the binary filter and the polyethylene wall. The dose at the surface of the sample was 32 Gy, and the dose rates varied depending on the LET.

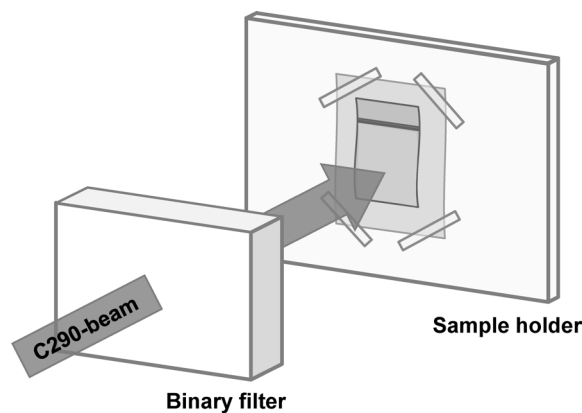


Fig. 2. A Schematic Drawing of the Experimental Setting for C290-Beam Irradiation at HIMAC

A reaction mixture was transferred into a polyethylene bag and attached as flat as possible onto the acrylic sample holder. Samples were irradiated by a C290-beam of arbitrary LET, adjusted using a binary filter with appropriate thickness.

X-Band EPR Measurement A 100 μL aliquot of irradiated reaction mixture was drawn into polytetrafluoroethylene (PTFE) tubing (i.d. 0.32 ± 0.001 inches, wall 0.002 ± 0.0005 inches; ZEUS, Orangeburg, SC, U.S.A.). The PTFE tubing was set in a TE-mode EPR cavity using a special quartz sample tube, and then measured by an X-band EPR spectrometer (JEOL, Tokyo). EPR conditions were as follows: microwave frequency, 9.4 GHz; microwave power, 2.00 mW; main magnetic field, 337.9 mT; field modulation frequency, 100 kHz; field modulation amplitude, 0.063 mT; time constant, 0.3 s; and magnetic field sweep rate, 2.5 mT/min.

For X-ray irradiated samples, EPR measurements were started approximately 3 min after irradiation, and repeated every 1 min for 10 min. The concentration time course of DMPO-OH was obtained for each sample. The concentration of DMPO-OH at the end of X-ray irradiation (time=0) was obtained by extrapolating the decay curve of DMPO-OH to time=0. Correcting for decay of DMPO-OH during the 32 Gy X-ray irradiation, which took 10 min, the net concentration of DMPO-OH was obtained according to the method described previously.⁶⁾ The concentration of DMPO-OH was calculated based on the EPR signal intensity of a standard (0.2 mM) TEMPOL solution measured with exactly the same geometry and parameters as above.

For the carbon-ion beam irradiated samples, a single EPR measurement was performed for each sample 20–60 min after irradiation, due to restricted usage time of HIMAC making repeated measurements for each sample difficult. Concentration of DMPO-OH at the end of the C290-beam irradiation was calculated correcting for the elapsed time after irradiation using the average decay rate of DMPO-OH obtained from the X-ray experiments. Decay correction was calculated with elapsed time=25 min for any samples which had an elapsed time after irradiation longer than 25 min. Decay of DMPO-OH during carbon-ion beam irradiation was not corrected for due to the irradiation time (2–5 min) being short.

Results and Discussion

Consistent with a previous report,⁷⁾ $\cdot\text{OH}$ and hydrogen radicals ($\cdot\text{H}$, just a hydrogen atom) were produced when aqueous samples were irradiated by X-rays or a C290-beam. Overlapping EPR spectra of DMPO-OH and DMPO-H ($\cdot\text{H}$ adduct of

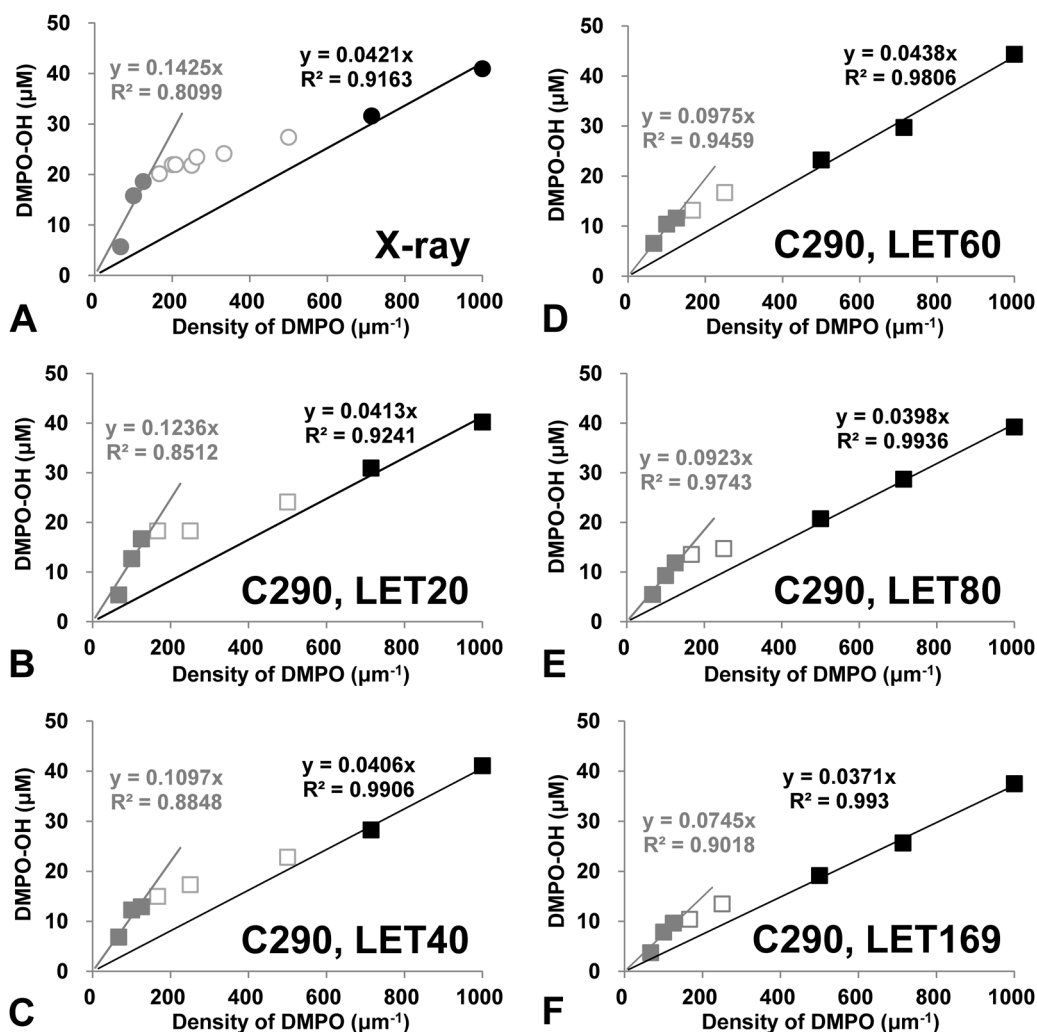


Fig. 3. Association between Initial Density of DMPO and Concentration of DMPO-OH Generated in the Irradiated Reaction Mixtures

Samples were irradiated with identical 32Gy doses of either (A) X-ray, (B) C290-beam with LET=20keV/ μm , (C) LET=40keV/ μm , (D) LET=60keV/ μm , (E) LET=80keV/ μm , or (F) LET=169keV/ μm . DMPO-OH/DMPO profiles showed three phases: the steep, linearly increasing phase (phase-1, gray marks), the plateau phase (phase-2, open marks), and another linearly increasing phase (phase-3, black marks) in all experiments.

DMPO) were observed in the DMPO-containing irradiated reaction mixture. To avoid contribution from the overlapping DMPO-H spectra, the 2nd line from the lower end of the magnetic field of the 4-line DMPO-OH EPR signal, which has minimum contribution from the DMPO-H spectra, was analyzed. DMPO-OOH (O_2^- adduct of DMPO) was not observed in this experiment.

The association between the concentration of DMPO added to the reaction mixture and the concentration of DMPO-OH generated after irradiation is shown in Fig. 3. Irradiation by X-ray (Fig. 3A) and five different C290-beam LETs (Figs. 3B–F) were tested. Table 1 shows the concentration, volume of space occupied, and molecule-to-molecule distance, as well as the linear density (on the track of the beam), which was defined as the reciprocal of molecule-to-molecule distance.

The concentration of DMPO-OH generated after irradiation increased with the initial concentration of DMPO. The profiles of increasing DMPO-OH generation showed three phases: the steep, increasing phase (phase-1, solid gray marks); plateau phase (phase-2, open marks); and another increasing phase (phase-3, solid black marks). A linear approximation through the origin was fitted to phase-1 (gray line) and phase-3 (black

Table 1. Relation of the Concentration, Volume of Space Occupied, Molecule-to-Molecule Distance, and the Linear Density (on the Track of the Beam)

Concentration (mM)	Volume of space occupied (nm^3)	Molecule-to-molecule distance (nm^a)	Linear density (μm^{-1}) ^b
1685 ^c	1.0	1.0	1000
600 ^c	2.8	1.4	714.3
208 ^c	8.0	2.0	500.0
61.6	27.0	3.0	333.3
30.0	55.4	3.8	263.2
26.0 ^c	63.9	4.0	250.2
15.0	110.7	4.8	208.3
13.3	124.9	5.0	200.0
7.7 ^c	215.7	6.0	166.7
3.3 ^c	503.2	8.0	125.0
1.6 ^c	1037.9	10	100.0
0.5 ^c	3321.2	15	66.7

^a) Molecule-to-molecule distance was calculated as the length of an edge of a cubic volume, which was occupied by one molecule. ^b) The linear density (on the track of the beam) was defined as the reciprocal of molecule-to-molecule distance. ^c) Concentrations used for C290-beam experiments.

line). The linear increase in DMPO-OH suggests that the concentration of DMPO in the reaction mixture was not sufficient in trapping all of the $\cdot\text{OH}$. This suggests that two different densities of $\cdot\text{OH}$ generation, *i.e.*, low and high, existed in this reaction system.

Furthermore, DMPO-OH generation *versus* the linear density of DMPO on the beam track reached a shoulder around $125\mu\text{m}^{-1}$ of DMPO density, corresponding to a DMPO concentration of 3.3mM , and then reached a plateau. This plateau suggests that the density of DMPO on the beam track in the reaction mixture was sufficient to trap the majority of generated $\cdot\text{OH}$. This suggests that the irradiation-induced sparse $\cdot\text{OH}$ are generated with a density corresponding to a concentration of 3.3mM or higher. The molecule-to-molecule distance at a concentration of 3.3mM is estimated to be approximately 8nm (Table 1).

The plateau of each plot in Fig. 3 was not completely horizontal, but gradually increased with increasing DMPO concentration. The DMPO-OH/DMPO plot has an additional steeply increasing region, which could be fit with a linear approximation through the origin. Such linear generation of DMPO-OH, proportional to the DMPO density and through the origin, implies an increased level of $\cdot\text{OH}$ generation. The highest concentration of DMPO tested in this study was 1685mM , which corresponds to a linear density of $1000\mu\text{m}^{-1}$ DMPO on the beam track (Table 1). The molecule-to-molecule distance at a concentration of 1685mM was estimated to be 1nm (Table 1). Therefore, a very high generation of $\cdot\text{OH}$ with a molecular distance of less than 1nm may be detected in this reaction system.

The highest concentration of generated DMPO-OH obtained using 1685mM DMPO, *i.e.*, linear density of $1000\mu\text{m}^{-1}$ DMPO on the beam track, was approximately $40\mu\text{M}$, similar between the X-ray and C290-beam irradiation conditions (Fig. 4A). The 32Gy dose used in this study may result in an identical amount of ionization and thus an identical amount of total $\cdot\text{OH}$ generated, independent of the source of radiation. Although the amount of DMPO-OH should reflect the amount of $\cdot\text{OH}$ scavenged, $40\mu\text{M}$ is markedly lower compared to the concentration of generated $\cdot\text{OH}$ expected above, *i.e.*, 3.3mM or 1.7M . The DMPO-OH concentration obtained by EPR measurement is an averaged concentration of the whole sample volume, suggesting that the $\cdot\text{OH}$ generation may be localized on the track of the radiation beam.

Photons, or X-rays in the present study, enter an object and travel a distance before interacting with molecules composing the object, in this case water. The traveling distance, *i.e.*, the range, of the photons are not identical, and decay exponentially. Initial interaction of a photon with an object results in another photon (scattered photon) and/or secondary electrons. These electrons lose their energy through repeated interaction, and are eventually stopped/absorbed. The range of the electrons depend on the electron energy and the material through which they travel. Taking into account such interactions of these resultant secondary electrons, the generation of $\cdot\text{OH}$ in water induced by X-rays as well as the secondary electrons may occur as frequently as every 8nm . In addition, dense generation of $\cdot\text{OH}$ may be due to a series of ionization/excitation by delta-rays, which are relatively higher energy electrons generated by interactions of secondary electrons; some clusters of dense $\cdot\text{OH}$ may be generated on the track of

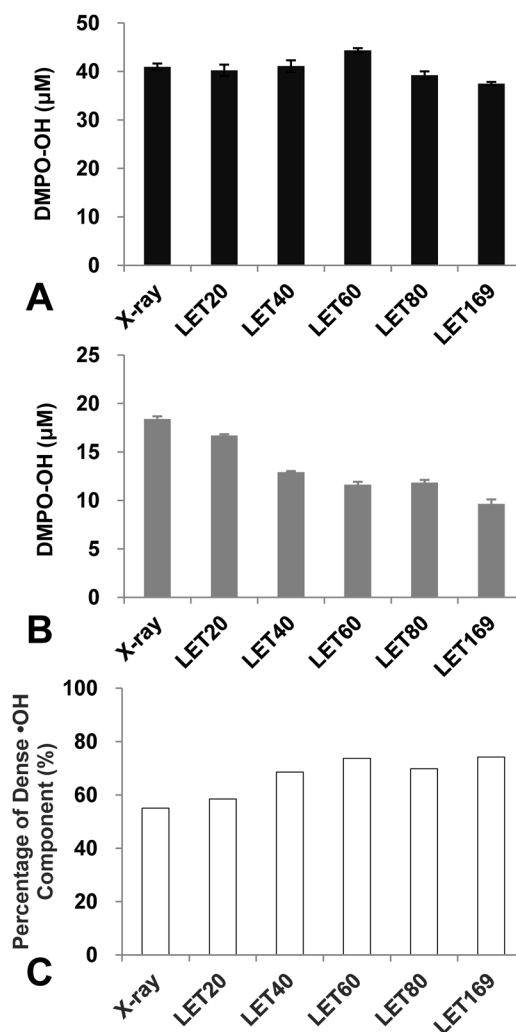


Fig. 4. Comparison of $\cdot\text{OH}$ Generation by Several Types of Irradiation

(A) Levels of total $\cdot\text{OH}$ generation, estimated by the DMPO-OH concentration obtained in reaction mixtures containing 1685mM DMPO. (B) Levels of sparse $\cdot\text{OH}$ generation, estimated by DMPO-OH concentration obtained in reaction mixtures containing 3.3mM DMPO, *i.e.*, the DMPO-OH levels at the shoulder. Reaction mixtures were irradiated by an identical 32Gy dose of several types of radiation. (C) Percentage of dense $\cdot\text{OH}$ generation, $(1-B/A)\times 100$.

these secondary electrons.

The level of DMPO-OH concentration at the shoulder, which reflects the sparse $\cdot\text{OH}$ concentration, was around $20\mu\text{M}$ with X-ray irradiation (Fig. 3A). The highest concentration of DMPO-OH detected using 1685mM ($1000\mu\text{m}^{-1}$) DMPO in this experiment was approximately $40\mu\text{M}$, which should reflect the total amount of $\cdot\text{OH}$. Therefore, the ratio of sparse and dense $\cdot\text{OH}$ components induced by X-ray irradiation could be expected as 50% of sparse $\cdot\text{OH}$ component, *i.e.* $\approx 3.3\text{mM}$, and 50% dense $\cdot\text{OH}$ component, *i.e.* $>1.7\text{M}$.

A biologically relevant dose of antioxidants or free radical scavengers may be able to partially scavenge the sparse $\cdot\text{OH}$ at a concentration of 3.3mM . Nevertheless, at low concentrations, most individual $\cdot\text{OH}$ may be unable to further react with other molecules, if no other organic molecules are in the vicinity. Highly reactive $\cdot\text{OH}$ are unable to travel significant distances due to reversion to water by reaction with its counterpart, the hydrogen radical ($\cdot\text{H}$). However, dense $\cdot\text{OH}$ generation can give rise to H_2O_2 and $\text{O}_2^{\cdot-}$ by reaction of two $\cdot\text{OH}$ and $\cdot\text{OH}$ with H_2O_2 , respectively. H_2O_2 and $\text{O}_2^{\cdot-}$ can travel

relatively long distances, resulting in further and more distant reactions. A biologically relevant dose of antioxidants may be unable to compete with the dense $\cdot\text{OH}$, H_2O_2 and O_2^- generated in dense $\cdot\text{OH}$ clusters, which may be scattered, can be regulated by a biological dose of antioxidants. Primary regulation of $\cdot\text{OH}$ is important for radioprotection, because $\cdot\text{OH}$ can be a source of other ROS. Balanced regulation of $\cdot\text{OH}$, O_2^- , and H_2O_2 may be very effective for protection from X-rays and other low LET radiation.

Highly charged (+6) carbon-ions may be able to ionize every water molecule on its linear track. In addition, some secondary electrons may be generated *via* this ionization process. The C290-beam-irradiated samples (Figs. 3B–F) also showed both sparse and dense $\cdot\text{OH}$ components, *i.e.* $\approx 3.3\text{ mM}$ and $>1.7\text{ M}$, respectively. The sparse and dense $\cdot\text{OH}$ generation may be due to interaction of the secondary electrons and primary ionizations, respectively. The level of DMPO-OH concentration at the shoulder, *i.e.*, the amount of sparse $\cdot\text{OH}$ generation, observed in the C290-beam experiments was lower compare to irradiation by X-ray, and the concentration of DMPO-OH at the shoulder decreased with increasing LET (Fig. 4B). DMPO-OH concentration at the shoulder was approximately $20\text{ }\mu\text{M}$ in the X-ray experiments, while it was $12\text{ }\mu\text{M}$ for $169\text{ keV}/\mu\text{m}$ LET. This result suggests that sparse ($\approx 3.3\text{ mM}$) $\cdot\text{OH}$ generation decreases with higher LET, or that the percentage of dense ($>1.7\text{ M}$) $\cdot\text{OH}$ generation increases with higher LET (Fig. 4C).

The molar concentration of 100% pure liquid DMPO was calculated to be 8.9 M , with a single DMPO molecule occupying 0.19 nm^3 , using the following considerations: purity of commercial DMPO, 99.0%; specific gravity, 1.01; and molecular weight of DMPO, 113.16 (Material Safety Data Sheet, Dojindo, Kumamoto, Japan). At a concentration of 1.7 M , one DMPO molecule is allocated a volume of 1 nm^3 . The remaining 0.81 nm^3 of this 1 nm^3 volume may be occupied by up to 27 water molecules. At a concentration of 1.7 M , one DMPO molecule, acting as a $\cdot\text{OH}$ detector, monitors only 27 vicinal water molecules. The spin-trapping efficiency of a DMPO molecule at 1.7 M may be close to 100%. At concentrations lower than 200 mM , in which the molecular distance of DMPO becomes longer than 2 nm , the spin-trapping efficiency of a single DMPO molecule should be lower due the majority of $\cdot\text{OH}$ being unable to reach the DMPO. The true averaged amount of sparse $\cdot\text{OH}$ generation may therefore be greater than that shown in Fig. 4B.

Carmichael *et al.* reported that the spin-trapping efficiency of DMPO for $\cdot\text{OH}$ was 35%.⁸⁾ In their experiment, several concentrations (max 440 mM) of DMPO solutions were irradiated by 136 Gy γ -ray. They obtained a plateau similar to the present study, and calculated a spin-trapping efficiency of 35% by comparing the maximum concentration of DMPO-OH measured at the plateau, $14.2\text{ }\mu\text{M}$, with the calculated $\cdot\text{OH}$ concentration, $40\text{ }\mu\text{M}$, obtained from the reported g -value. This observation probably reflects only the sparse component of $\cdot\text{OH}$ generation. Factors which may affect the spin-trapping efficiency are the probability of meeting a spin-trapping agent with a subject-free radical and the reactivity between them. The molecule-to-molecule reactivity should be identical, therefore only the probability of meeting a spin-trapping agent with a subject-free radical, *i.e.*, the molecular distance between them, can affect the [DMPO-OH]/[DMPO] profile. In

other words, the profile of [DMPO-OH]/[DMPO] depends on whether an $\cdot\text{OH}$ can reach a DMPO molecule without reacting with other molecules.

Track structures reported for heavy-ion beams are composed of a core and penumbra.⁹⁾ The X-ray-like $\cdot\text{OH}$ generation can be expected to be in the penumbra region, with much denser $\cdot\text{OH}$ generation in the core. When biological molecules are in the vicinity of the track of the C290-beam, the effect of dense $\cdot\text{OH}$ generation at the core region, *i.e.* $>1.7\text{ M}$, may be hardly distinguishable from the direct action of the radiation. A biologically relevant dose of antioxidants may not be able to completely inhibit such dense $\cdot\text{OH}$ production. The oxygen effect may not be expected for such dense $\cdot\text{OH}$ generation, since some of dense $\cdot\text{OH}$ can definitely cause a reaction with the biological molecules on the track. Even if the generation of $\cdot\text{OH}$ required water, such dense $\cdot\text{OH}$ may behave as direct action. Since dense $\cdot\text{OH}$ generation can give rise to O_2^- and H_2O_2 , regulation of O_2^- and H_2O_2 may be effective in suppressing the indirect ionization of the C290-beam rather than primary regulation of $\cdot\text{OH}$.

Conclusion

Irradiation of an aqueous solution by ionizing radiation can generate $\cdot\text{OH}$ of local concentrations of 3.3 mM or more. This corresponds to generation of radicals at a molecular distance of 8 nm or shorter, and likely is eccentrically-localized on the beam track. Extremely dense generation of $\cdot\text{OH}$ at concentrations above 1.7 M , corresponding to a linear density of every 1 nm or shorter on the beam track, may also be expected. The percentage of dense $\cdot\text{OH}$ generation increased with increasing LET. Different types of dense $\cdot\text{OH}$ generation may be expected for X-ray and C290-beams.

Acknowledgments The authors are grateful to the staff of the HIMAC for their help in irradiating samples by the carbon-ion beam. This work was supported by JSPS KAKENHI Grant Number 23591853.

Conflict of Interest The authors declare no conflict of interest.

References

- 1) Furusawa Y., Fukutsu K., Aoki M., Itsukaichi H., Eguchi-Kasai K., Ohara H., Yatagai F., Kanai T., Ando K., *Radiat. Res.*, **154**, 485–496 (2000).
- 2) Kamada T., *Int. J. Clin. Oncol.*, **17**, 85–88 (2012).
- 3) Matsumoto K., Nagata K., Yamamoto H., Endo K., Anzai K., Aoki I., *Magn. Reson. Med.*, **61**, 1033–1039 (2009).
- 4) Matsumoto K., Aoki I., Nakanishi I., Matsumoto A., Nyui M., Endo K., Anzai K., *Magn. Reson. Med. Sci.*, **9**, 131–140 (2010).
- 5) Matsumoto A., Matsumoto S., Sowers A. L., Koscielniak J. W., Trigg N. J., Kuppusamy P., Mitchell J. B., Subramanian S., Krishna M. C., Matsumoto K., *Magn. Reson. Med.*, **54**, 1530–1535 (2005).
- 6) Ueno M., Nakanishi I., Matsumoto K., *J. Clin. Biochem. Nutr.*, **52**, 95–100 (2013).
- 7) Moritake T., Tsuboi K., Anzai K., Ozawa T., Ando K., Nose T., *Radiat. Res.*, **159**, 670–675 (2003).
- 8) Carmichael A. J., Makino K., Riesz P., *Radiat. Res.*, **100**, 222–234 (1984).
- 9) Muroya Y., Plante I., Azzam E. I., Meesungnoen J., Katsumura Y., Jay-Gerin J. P., *Radiat. Res.*, **165**, 485–491 (2006).